We are IntechOpen, the world's leading publisher of Open Access books Built by scientists, for scientists

6,900
Open access books available

186,000
International authors and editors

200M
Downloads

Our authors are among the

154
Countries delivered to

TOP 1%
most cited scientists

12.2%
Contributors from top 500 universities

WEB OF SCIENCE™

Selection of our books indexed in the Book Citation Index in Web of Science™ Core Collection (BKCI)

Interested in publishing with us?
Contact book.department@intechopen.com

Numbers displayed above are based on latest data collected.
For more information visit www.intechopen.com

Chapter

Equilibrium Structures and Stationary Patterns on Magnetic Colloidal Fluids

Ricardo Peredo Ortíz, Martin Hernández Contreras and Raquel Hernández Gómez

Abstract

In this chapter, we review the experimental and theoretical modeling of structural and dynamical properties of colloidal magnetic fluids at equilibrium. Presently, several prototype experimental systems are very well characterized. We survey the different models, which help to reach a comprehensive knowledge of these complex magnetic fluids. One prime example is the ongoing investigation of the realistic interparticle potentials that drive the formation of the different phase states observed experimentally. Further, a stochastic equation approach for the description of tracer diffusion, viscoelasticity, and dielectric relaxation at equilibrium in colloidal ferrofluids is discussed.

Keywords: ferrofluids, viscoelasticity, colloidal magnetic fluids, magnetohydrodynamics, dielectric relaxation, diffusion stochastic dynamics

1. Introduction

Colloidal magnetic fluids are made up of nanometer and micron-size ferromagnetic particles dispersed either in electrolytes or in organic solvents [1]. Due to their easy manipulation with magnetic or electric fields, they are having a significant impact on diverse technological applications ranging from biomedicine [2] and photonic devices [3, 4] up to fundamental studies that motivate the development of modern theories of nonequilibrium condensed matter [5–10]. In this chapter, we review the studies of static structural and dynamical properties in colloidal magnetic fluids, which provide a comprehensive description of their bulk phase behavior at thermal equilibrium. Presently, model magnetic colloidal systems can be prepared with tunable interaction among particles of the hard sphere and long-range dipolar types [11–14], especially the colloidal system constituted of micron-size polystyrene spheres that are electrically charged and dispersed in organic solvents [11]. In such a system, particles acquire an induced electric dipole moment under the external static electric field. Confocal microscopy has allowed the determination of its three-dimensional bulk phase diagram as a function of applied electric field and by taking into account the presence of a 1:1 salt. The electric and magnetic dipole pair interaction potential is symmetric. Consequently, a corresponding change of physical units leads to an equivalent description of the magnetic fluid phase diagrams. Novel Monte Carlo simulation methods have

confirmed the different experimental phases [15, 16]. Integral equations and density functional theories have assisted in the understanding of the phases formed by molecular liquids [17], and they have been used to gain qualitative insight into the expected phases as a function of volume fraction and dipolar strength of colloidal magnetic fluids [18–23]. Likewise, the structure factor and diffusion coefficient of magnetic suspensions made of maghemite nanoparticles dispersed in water and equilibrium with electrolyte solutions have also been reported [24–31]. The measured structure factor provides the microscopic arrangements of particles accurately. Here, we provide a Langevin stochastic approach that allows the determination of the translational and rotational diffusion of the particles in ferrofluids [32, 33]. These dynamic properties, in turn, allow quantifying the viscoelastic and dielectric moduli of the structural evolution of the fluid toward their equilibrium states [34]. This approach may help to interpret recent experiments of passive microrheology [35, 36] and Altern Current spectroscopic techniques that measure the viscoelastic dynamics and dielectric relaxation of colloidal magnetic fluids. It is expected these theoretical methods be extended to help to understand the corresponding experimental observations of similar dynamics in two-dimensional paramagnetic colloids [37] and under external fields.

2. Experimental observations of structural properties of magnetic fluids

The importance of knowing the phase diagram of a ferrofluid resides on the information it provides about the undetermined underlying effective interaction of the ferromagnetic particles [13]. For maghemite nanoparticles in aqueous solutions, there have been attempts to determine such electrostatic potentials by using the measured parameters such as dipole strength and fluid density as inputs in Brownian dynamics simulations to reproduce the observed bulk structure factor [30, 31].

2.1 Importance of an experimental phase diagram of maghemite colloid

There is a set of experiments in a well-characterized system of electrically stabilized maghemite nanometer-size particles, which are dispersed in water [24–29]. Its stabilization is reached with the citrate electrolyte. By fine-tuning the salt concentration, the particle's interaction was shifted from repulsive, where they form a solid glass phase, into long-range attractive interactions that yield a fluid or gas state behavior. These experiments have prompted the determination of the corresponding pairwise interaction among particles [13]. The proposed interaction consists of a Yukawa repulsive part, a Van der Waals short-range attraction and includes an angular averaged attractive long-range pair dipole potential. There have not been attempts to predict the phase diagram with these potentials. However, the modeled interactions were used to determine with Brownian dynamics the observed structure factor [30, 31]. By using a generic model of pair dipole interactions together with an effective attraction associated with density gradients, Lacoste, et al. [38] considered a quasi-two-dimensional layer of a dilute ferrofluid subjected to a perpendicular magnetic field, and with the help of a mean field energy approach, they found modulated phases given by stripes and hexagonal formations. The Gibbs free energy they considered for inhomogeneous systems has the general shape $G = F_H - \mu\phi\left(\vec{r}\right)$, where F_H is the Helmholtz energy; the chemical potential μ constrains the average local composition $\phi\left(\vec{r}\right)$ or space-dependent

volume fraction of particles at the position $\vec{r}$ to have a total fixed value $\int dr^2 \phi\left(\vec{r}\right)$. Their model is a thin film of ferrofluid with a constant magnetic field acting perpendicular to the fluid layer. Since external fields produce an inhomogeneous distribution of particles, the volume fraction becomes a local function of position. F_H is constructed at mean field level to have the following terms: the internal energy of the pair dipole-dipole interactions $(1/2)\sum_{i,\, j(i\neq j)} V_{dd}\left(\vec{r}_{ij}\right)$ and the rotational free energy F_{rot} of an ideal gas of paramagnetic dipoles with polar angles as the only degrees of freedom under a constant magnetic field. F_{rot} is obtained from the partition function in the canonical ensemble calculated with the total energy of dipole $\hat{m}_i$ with field $\vec{H}$ interactions $-\sum_i \hat{m}_i \cdot \vec{H}$, the entropic energy contribution due to all possible spatial configurations of the finite size particles in the volume available $-k_B T[\phi \ln \phi + (1-\phi)\ln(1-\phi)]$ as given by the lattice gas. k_B is the Boltzmann constant and the room temperature T. The energy of particles that arise from gradients in their concentration and therefore setting their average available local volume is $(1/2)\int dr^2 \left[\nabla \phi\left(\vec{r}\right)\right]^2$, which is provided by a continuous version of the lattice gas model. The ferroparticles are all equal, and their energy of pairwise interaction for two dipoles separated with the center-to-center vector distance $\vec{r}$ is given by $V_{dd} = -\left(m^2/r_{ij}{}^4\right)\left[3\vec{r_{ij}} \cdot \hat{u}_i \vec{r_{ij}} \cdot \hat{u}_j - \hat{u}_i \cdot \hat{u}_i\right]$, where m is the particle's constant dipole moment, and $\hat{u}_i$ is the unitary vector orientation of particle i. Thus, the resulting mean Gibbs energy G is mapped from the lattice gas model into a continuous position dependence representation. The free energy is a function of the local dipole moment and concentration $m(r)$, $\phi(r)$. A ferrofluid in a continuous single phase such as a dispersed homogenous ferrofluid is an equilibrium state with an average concentration $\overline{\phi}$ and bulk dipole moment $\overline{m}$. This state is characterized by the minimum of the free energy, that is, $\partial G/\partial m = 0$, $\partial G/\partial \phi = 0$, which provides the average values of bulk dipole moment and concentration above. However, it is observed that for specific magnitudes of the external field and ferrofluid concentration, there appears chaining of particles that coalescence into sheets, which at higher field strength evolve to labyrinthine structures. The nucleation of these structures starts with the formation of magnetization domains associated with small clustering of particles with sizes on the order of a few microns. Short-wavelength thermal fluctuations of this size are capable of describing the formation of nonuniform phases. One way to analyze the formation of these phases uses the expansion of the free energy difference [38] $\Delta G(\varphi, m) = G(\varphi, m) - G(\overline{\varphi}, \overline{m})$ up to second order in the fluctuations of dipole magnetization $\delta m = m(r) - \overline{m}$, and concentration $\delta\phi = \phi(r) - \overline{\phi}$ about their mean values. In the two-dimensional Fourier space representation, the free energy difference is a quadratic form $\Delta G = (1/2\pi^2)$ $\int d^2\, \vec{k}\, \left[a\left|\delta m\left(\vec{k}\right)\right|^2 + b\delta m\left(\vec{k}\right)\delta\phi\left(-\vec{k}\right) + c\left|\delta\phi\left(\vec{k}\right)\right|^2\right]$ with a, b, c related to the material parameters of ferrofluid external field $\overline{m}$ and $\overline{\phi}$. The uniform phase becomes unstable to the formation of modulated nonuniform phases if the determinant of the integrand gets negative at the minimum of wave number [38].

It has been recognized that ferromagnetic particles of 10 -nm size remain dispersed [39]; however, when particles have larger sizes up to the micron scale, experiments find they do assemble into chains, rings, and nets were several chains bound together into an amorphous structure [40]. A mean field theory that takes into account such topological structures was developed to explain the liquid-gas phase transition by the formation of Y-like bounds of chains in the network [41]. There remains a quantitative verification of this theory with its experimental

counterpart and with computer simulations. Another method to validate the proposed model of particle's interaction is based on the parameters that appear in the Lennard-Jones potential that represents the Van der Waals attractions together with the pair dipole-dipole potential, and by fitting the predicted magnetization curve as a function of the applied magnetic field to the experimental one [42]. Even though there is not yet a realistic model interaction potential that represents the interaction of ferromagnetic particles, the use of fitting parameters as mentioned above has led to the prediction of the structure factor and the birefringence as a function of the applied field, which shows qualitative agreement with the experimental values [22, 29–31].

2.2 Experimental phase diagram of a charged and sterically stabilized electrorheological colloidal suspension under an electric field

Yethiraj et al. [11] made a colloidal system of charged and sterically stabilized polymethyl methacrylate spheres of micron size in an organic solvent to have dipole moments on particles induced by an electric field. This monodisperse suspension shows both long-range repulsion, and attractive anisotropic interaction potential that is fixed with the addition of salt, whereas the dipolar interaction is controlled by the external electric field. For low Reynolds numbers and in an infinite fluid, a solid spherical particle that sinks in the fluid reaches a terminal velocity due to a balance of the friction force exerted by the fluid that opposes the gravitational force on the particle. If the fluid has a dynamic viscosity η and mass density ρ_f, and the spherical particle possesses a mass density ρ_m, then the steady velocity is $V = \left(\rho_f - \rho_m\right)gd^2/18\eta$, where g is the gravitational acceleration and d the particle diameter. Thus, the effect of gravity is diminished by matching the density of the particles to that of the solvent. The Van der Waals attraction that otherwise would produce aggregation was reduced by matching the index of refraction to the visible. The Van der Waals attractive energy of two spherical particles is $V_{vdw}(r) = -(A/12)\left[d^2/\left(r^2 - d^2\right) + d^2/r^2 + 2\ln\left(1 - d^2/r^2\right)\right]$, where r is the separation distance of the spheres' centers [43]. Therefore, the Hamaker constant [44] $A = 3h\nu\left(n_p - n_s\right)^2\left(n_p + n_s\right)^2/16\sqrt{2}\left(n_p{}^2 + n_s{}^2\right)^{3/2}$ can be made zero if the optical refractive index of the colloidal particles n_p is equal to that of the solvent n_s for an appropriated selection of the frequency ν of the visible light. Here, h is the Planck constant. With confocal microscopy studies, they observed in real-space representation crystalline structures controlled by the repulsive part of the potential, which induces a structure of random hexagonal close packing. For longer-range repulsion, it becomes face-centered cubic (fcc), and one can also find a body-centered cubic phase (bcc). As a function of the electric field, a dipolar phase diagram was established. For low field, there is a sequence of fluid-bcc-fcc (phase-centered cubic) phases. For larger values of the field, there is string formation that coalesces into sheets that in turn coarsen to form body-centered tetragonal crystallites. Moreover, for increasing volume fractions, the string fluid crystallizes to a space-filling tetragonal phase. Such a rich variety of phases can be generated controllably by the concentration of the electrolyte. High salt concentration screens the electrostatic repulsion becoming short-distance hard sphere interaction whereas the small content of salt increases the spatial range of the potential. The dipolar interaction is controlled by the external electric field. Consequently, due to the symmetric form of the electric and magnetic dipolar potential, a simple change of physical units leads to the similar conclusions to be expected for a colloidal magnetic ferrofluid. For oily ferrofluids, the short-range Van der Waals attraction and hardcore repulsion are modeled by the

Lennard-Jones interaction energy $V_{LJ}(r) = 4\varepsilon_0\left[(d/r)^{12} - (d/r)^6\right]$ with ε_0 the potential depth that can be estimated experimentally. For ferrofluid in an aqueous solvent of dielectric constant ε and monodisperse spherical particles, due to the presence of salt at density ρ_i, the Yukawa potential $V_{yuk}(r) = Q^* \exp[-\kappa(r-d)]/r$, $\kappa^2 := 4\pi e^2\rho_i/\varepsilon k_B T$ is used instead, where e is the electron charge. Q^* is the effective electric charge of a particle that can be measured with electrophoresis experiments.

2.3 Theoretical models of phase diagrams of dipolar colloidal fluids: computer simulation and optimization techniques

Finite-temperature calculations of ground state free energies with Yukawa repulsion and dipolar-dipolar interactions of varying strength were performed by Hynninen and Dijkstra [15]. In their calculations, they used canonical Monte Carlos simulations to obtain the free energy minimum as a function of volume fraction and dipolar strength in three-dimensional model systems. They found a phase diagram that contains the same phases as was observed by Yethiraj et al. [11]. However, additionally, they predicted a new hexagonal close-packed phase at the hard sphere repulsion limit and body-centered orthorhombic when the repulsion becomes long range by lowering the content of electrolyte in solution. Their method allows quicker and reliable determinations of the three-dimensional phase diagram than the evolutionary algorithm method that searches for the ground state at zero temperature for two-dimensional systems [45]. The bulk phase diagram has not been searched yet with genetic algorithm (GA) at finite temperature. A particular detail of GA is that to look for the minimum of the free energy, the derivative of the energy function at each evolution step is required for finding the best-adapted crystal structures (individuals) in the population, which is made up of several crystal structures produced by the algorithm. The search of the best-adapted individuals (crystal phase) is done in the energy landscape. For fixed pressure and finite temperature, the Gibbs free energy as a function of pairwise interaction strength and particles concentration in the fluid yields a three-dimensional plot of the free energy known as energy landscape, which has local minima and maxima. The global minimum of an equilibrium crystal structure is reached with the assistance of a local gradient algorithm that requires the derivative of the energy. Such a procedure makes an indirect search of the crystal structure by sampling the energy landscape. Thus, it becomes technically more involved to implement than the Hynninen et al. method of MC ground state energy searches. In **Figure 1**, we provide two nonequilibrium states of local minima that result from the application of a genetic algorithm approach at zero temperature and fixed pressure.

Recently, Spiteri and Messina [16] have proposed an efficient nonlinear optimization technique that allows predicting the crystal phases of dipolar colloids at zero temperature without the need to use derivatives of the free energies. It was found that for a monodisperse repulsive hard sphere plus dipole-dipole interaction, the predicted phase diagram has the same phases as was previously found by Hynninen et al. [15] and that a knew so-called clinohexagonal prism span all known ground state structures at any density. There remains to be verified if this prediction fulfills at a finite temperature also.

2.4 Experimental structure factors and diffusion coefficients

The microstructural order inside of the ferrofluid is determined by the potential interaction among particles. The measured structure factor yields the details of the particles' spatial geometric arrangement. The water-based maghemite ferrofluid is

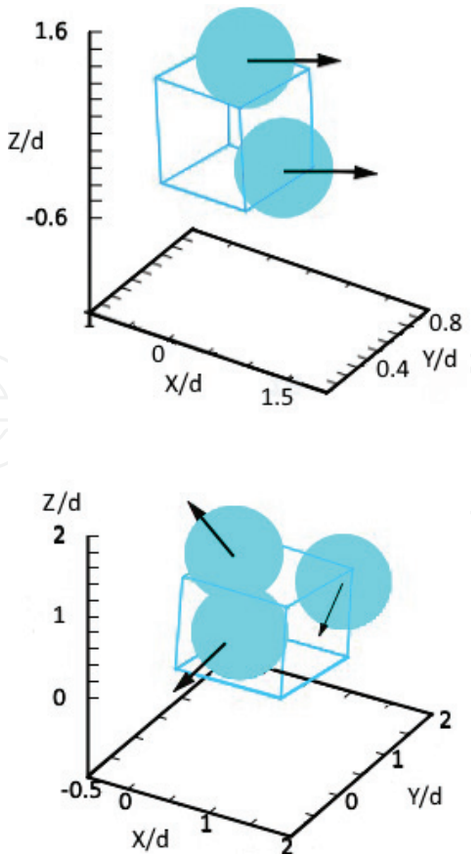

Figure 1.
Genetic algorithm prediction of minimum local structures at two densities of equally sized ferroparticles in the aqueous colloidal magnetic fluid at $T = 0K$ and constant pressure. X, Y, and Z are Cartesian coordinates. Both structures are simple cubic cells. The bottom structure has the highest density and the lowest enthalpy energy. Black arrows depict the direction of the particle's dipole moment.

electrostatically stabilized. The interparticle interaction was modeled in Ref. [13] with a Yukawa repulsion part together with the anisotropic dipolar potential. The highest peak of the structure factor regarding wave number k, as a function of applied field, shows the same qualitative tendency as the experimental peak. For the same type of pair potential, a calculation of the structure factor using the rescaled mean spherical approximation of liquid theory was developed by Wagner et al. [46]. Their calculated structure factor compares well with the measured one in a cobalt-based aqueous colloid. Their fabricated ferrofluid has a polydispersity in particle sizes, which were successfully taken into account via a Shultz distribution. The microstructure in the suspension has also been modeled by Pyanzina et al. [47] with an analytical pair correlation function obtained through a thermodynamic expansion of the density and dipole strength. They find excellent agreement between the theoretical calculation and molecular dynamics data for the scattering vector dependence of the pair correlation at the dilute limit. The agreement improves at low volume fraction whereas at higher concentrations, the coincidence occurs only about the main first peak. Recently, we determined with Langevin dynamics simulations the structure factor in model monodisperse ferrofluids of spherical particles that interact through Lennard-Jones plus dipolar pair potentials. As previously found [17, 42], we also find that at the low colloid density and dipole strength, the particles are well dispersed; however, for higher dipole moment, there is chaining of particles. If the concentration rises, then the system shows a small cluster with few particles as can be seen in **Figure 2** of the structure factor $S(k)$.

The contact values at k = 0 yield the compressibility modulus. The material parameters of maghemite colloid were used [40]. At low densities and magnetic moment, there is liquid order. For higher dipole moments, formation of chain appears.

Figure 3 is a plot of the collective diffusion coefficient D_C normalized to the free diffusion of a single particle D^0 in the hydrodynamic limit of zero wave number. It is given as $D_c = D^0/S(k=0)$. In the left-hand side plot of **Figure 3(a)** with symbol ∘ the collective diffusion coefficient increases as the magnitude of dipole moment increases at high-density limit of $\rho^* = 0.9$. However, a reverse behavior is shown by this collective diffusion property when the density is very low $\rho^* = \rho d^3 = 0.1$ (plot with a symbol ●, $\rho = N/V$, N the number of particles, and V the volume of the fluid). We should note that in the former case, there occurs the formation of chains, and at the highest concentration, the particles are dispersed.

The researchers in Ref. [46] also measured the wave vector-dependent collective translational diffusion coefficient in the absence of an external field using X-ray

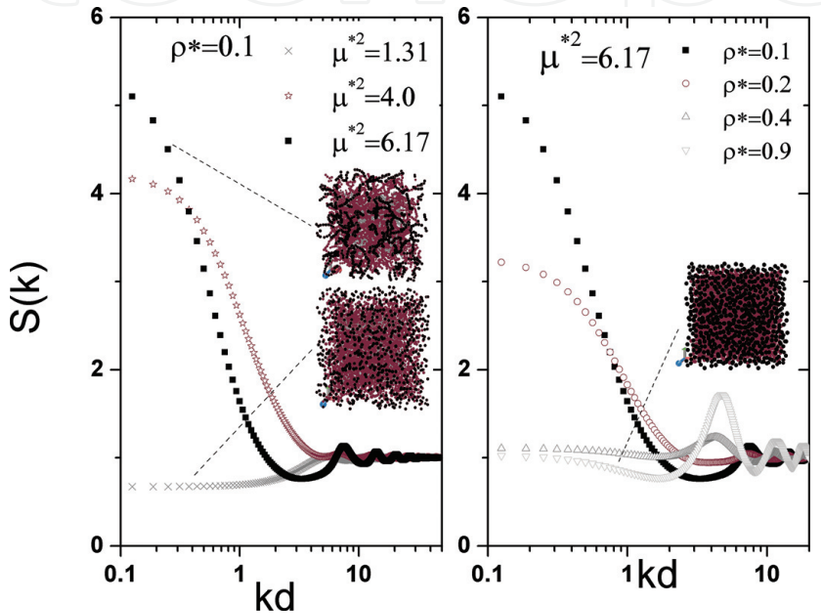

Figure 2.
Simulation results of structure factor versus wave number. The contact values at k=0 yield the compressibility modulus. The material parameters of maghemite colloid were used [40]. At low densities and magnetic moment, there is liquid order. For higher dipole moments formation of chain appears.

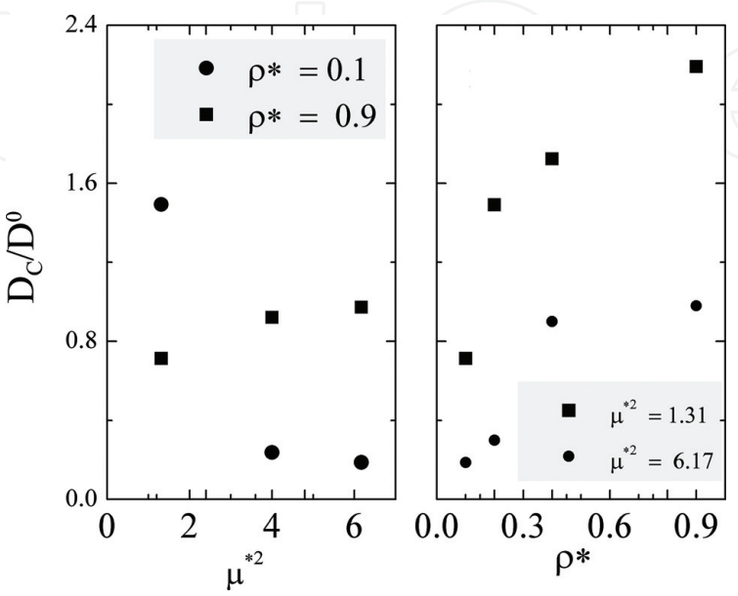

Figure 3.
Calculated collective diffusion coefficient D_c normalized to the free particle diffusion constant at the hydrodynamic limit of low wavenumber k = 0. Notice that at high density, $\rho^* = 0.9$, this property increases (left, black square symbol).

correlation spectroscopy. Such a dynamical property has a known linear dependence on the particles' hydrodynamic interactions (HIs). The proposed theoretical hydrodynamic function that captures the HI among particles overestimates the experimental data. On the other hand, Meriguet et al. [29] used small-angle neutron scattering to measure the incoherent scattering function at the fixed magnetic field. The incoherent part gives in the long-time overdamped regime, the single translational diffusion coefficient for long wave vectors k, and the coherent part provides the collective diffusion as a function of k. Using liquid theory definitions of these two dynamical functions, their comparison with the experimental values yields good agreement at all wave scattering vectors k. The same collective diffusion coefficient can be measured by forced Rayleigh scattering also [26]. In this technique, the fluctuations in concentrations of the particles are considered a dynamic variable. We note that similar studies have been undertaken in the case of rodlike macromolecules in suspension such as Tobacco mosaic virus [48]. Explicit statistical mechanics derivations for the dynamical collective correlation functions (intermediate scattering function) have been given that fit well Brownian dynamics simulations just at long wave numbers but fail at intermediate and short k values. In Refs. [32–34], we proposed a Langevin equation theory for a tracer ferroparticle whose motion is coupled to the cloud of the other colloidal magnetic particles with which it interacts.

$$\begin{aligned} M\frac{dV(t)}{dt} &= -\zeta^0 \cdot V(t) - \zeta^0_{TR} \cdot W(t) + f^0(t) + F(t), \\ I \cdot \frac{dW(t)}{dt} &= -\zeta^0_R \cdot W(t) - \zeta^0_{RT} \cdot V(t) + t^0(t) + T(t). \end{aligned} \tag{1}$$

V, W are the translational and angular velocities of the tracer particle and referred to a space-fixed frame at the center of mass of the tracer and following the orientation of the main tracer axis of symmetry. M and I are the mass and particle's matrix of the moment of inertia, respectively. There are neither hydrodynamic interactions among particles nor external magnetic fields. The first two terms in Eq. (1) are the solvent friction force and torque. The short-time free particle diagonal friction tensors ζ^0, ζ^0_{TR}, ζ^0_{RT}, ζ^0_R represent hydrodynamic drag forces and torques. These friction and random forces are the only quantities that convey information on the nature of the solvent. They need to be measured experimentally or provided by a free parameter. Moreover, they ignore the molecular degrees of freedom of position and orientation coordinates and momenta. They are coupled to the thermally driven solvent random forces f^0 and torques t^0 by fluctuation-dissipation theorems [32–34]. The total force and torque F, T on the tracer by the rest of the colloidal particles, which are at the concentration $n\left(\vec{r},\Omega,t\right) = \sum_{i=1}^{N}\delta\left(\vec{r}-\vec{r}_i(t)\right)\delta(\Omega-\Omega_i(t))$, are given by

$$\begin{aligned} F(t) &= \int d^3\,\vec{r}\; d\Omega \nabla\psi\left(\vec{r},\Omega\right) n\left(\vec{r},\Omega,t\right), \\ T(t) &= \int d^3\,\vec{r}\; d\Omega\left[\vec{r}\times\nabla + \nabla_\Omega\right]\psi\left(\vec{r},\Omega\right) n\left(\vec{r},\Omega,t\right) \end{aligned} \tag{2}$$

with $\Omega = (\theta,\varphi)$ being the polar angles, $\psi\left(\vec{r},\Omega\right) = V_{LJ} + V_{dd}(\mu_0/4\pi)$ is the pair potential with μ_0 the magnetic permeability of vacuum, and $\nabla_\Omega = \hat{u}\times d/d\hat{u}$ the angular gradient operator. The total force and torque are calculated using the probe's dipole located along the Z axis direction of its local frame, that is $\Omega = (0,0)$. The unitary Cartesian vector $\hat{u}$ of the orientation of any other particle is in the direction of that particle's axis of symmetry. The Langevin equation is coupled to the diffusion

equation of the concentration of particles around the tracer through the total force on the tracer, which is linear in the instantaneous concentration of particles.

$$\overleftrightarrow{M}\cdot\frac{d\overleftrightarrow{V}(t)}{dt}=-\overleftrightarrow{\zeta}^{0}\cdot\overleftrightarrow{V}(t)+\overleftrightarrow{f}(t)+\int d^{3}\,\vec{r}d\Omega\overleftrightarrow{\nabla}\,\left[\psi\left(\vec{r},\Omega\right)\right]n\left(\vec{r},\Omega,t\right)\tag{3}$$

Here, $\overleftrightarrow{V}=(V,W)$, $\overleftrightarrow{\nabla}=\left(\nabla,\vec{r}\times\nabla+\nabla_{\Omega}\right)$. and the diffusion equation of the concentration $\partial n\left(\vec{r},\Omega,\mathrm{t}\right)\Big/\partial t=-\nabla\cdot\left[\overleftrightarrow{V}\,n(t)\right]$ can be linearized altogether with Eq. (3) in $\delta\mathrm{n}(\mathrm{t})=\mathrm{n}(\mathrm{t})\text{-}\mathrm{n}^{eq}\left(\vec{\mathrm{r}},\Omega\right)$ around the local equilibrium concentration of particles $\mathrm{n}^{eq}\left(\vec{\mathrm{r}},\Omega\right)\coloneqq\left\langle n\left(\vec{r},\Omega,t\right)\right\rangle$. Thus, in the center of mass of the tracer, and using general results of linear irreversible thermodynamics, the diffusion equation reads

$$\begin{aligned}\frac{\partial\delta n\left(\vec{r},\Omega,t\right)}{\partial t}&=\left[\overleftrightarrow{\nabla}n^{eq}\left(\vec{r},\Omega\right)\right]\cdot\overleftrightarrow{V}-\int_{0}^{t}dt'\int d^{3}\vec{r}'d\Omega'\int dr''d\Omega''L\left(\vec{r},\vec{r}',\Omega,\Omega';t-t'\right)\\&\quad\times\sigma^{-1}\left(\vec{r}',\vec{r}'',\Omega',\Omega''\right)\delta n\left(\vec{r}'',\Omega'',t'\right)+\overleftrightarrow{\nabla}\cdot j\left(\vec{r},\Omega,t\right).\end{aligned}\tag{4}$$

where the Onsager coefficient $L=\left\langle\overleftrightarrow{\nabla}\cdot j\left(\vec{r},\Omega,t\right)\cdot\overleftrightarrow{\nabla}\cdot j^{\dagger}\left(\vec{r},\Omega,t\right)\right\rangle$ is related to the spatial variation of the stochastic current $j\left(\vec{r},\Omega,t\right)$. † means transpose and complex conjugate (adjoint operator). The inverse of the static correlation function σ fulfills a relationship with the potential and concentration function [32–34]. Using methods of Green functions Eq. (4), one solves for $\delta n\left(\vec{r},\Omega,t\right)$, and the result is further substituted into the linearized version in the concentration of Eq. (3) yielding the tracer Langevin equation

$$\overleftrightarrow{M}\cdot\frac{d\overleftrightarrow{V}(t)}{dt}=-\overleftrightarrow{\zeta}^{0}\cdot\overleftrightarrow{V}\,(t)+\overleftrightarrow{f}(t)-\int_{0}^{t}dt'\Delta\,\overleftrightarrow{\zeta}\,(t-t')\cdot\overleftrightarrow{V}(t)+\overleftrightarrow{F}(t)\tag{5}$$

$\overleftrightarrow{F}$ are fluctuating forces arising from the spontaneous departure from zero of the net force and torque on the tracer. It satisfies the fluctuation-dissipation relationship with the tracer-effective friction coefficient $\left\langle\overleftrightarrow{F}(t)\overleftrightarrow{F}^{\dagger}(0)\right\rangle=k_{B}T\Delta\,\overleftrightarrow{\zeta}(t)$. $T=300K$ is the room temperature. As a result, explicit expressions for the tracer translational and rotational friction coefficients are given regarding the equilibrium concentration $\mathrm{n}^{eq}\left(\vec{\mathrm{r}},\Omega\right)$ that embodies the microstructure of the particles inside of the liquid, and the direct pair potential ψ,

$$\begin{aligned}\Delta\overleftrightarrow{\zeta}(t)&=\frac{k_{B}T}{(4\pi)^{2}}\int d^{3}\vec{r}d^{3}\vec{r}'d^{3}\vec{r}''d\Omega d\Omega'd\Omega''\left[\overleftrightarrow{\nabla}n^{eq}\left(\vec{r},\Omega\right)\right]\\&\quad\times\sigma^{-1}\left(\vec{r},\vec{r}',\Omega,\Omega'\right)\chi\left(\vec{r}',\vec{r}'',\Omega',\Omega'',t\right)\left[\overleftrightarrow{\nabla}''n^{eq}\left(\vec{r}'',\Omega''\right)\right]^{\dagger}.\\\Delta\overleftrightarrow{\zeta}\,(t)&=\frac{1}{k_{B}T(4\pi)^{2}}\int d^{3}\vec{r}d^{3}\vec{r}'d^{3}\vec{r}''d\Omega d\Omega'd\Omega''\left[\overleftrightarrow{\nabla}\psi\left(\vec{r},\Omega\right)\right]\\&\quad\times\chi\left(\vec{r},\vec{r}',\Omega,\Omega',t\right)\sigma\left(\vec{r}',\vec{r}'',\Omega',\Omega''\right)\left[\overleftrightarrow{\nabla}''n^{eq}\left(\vec{r}'',\Omega''\right)\right]^{\dagger}\end{aligned}\tag{6}$$

The propagator χ is obtained from the diffusion Eq. (4), and it is related to the van Hove function $C\left(\vec{r},\Omega,\vec{r}',\Omega',t\right) \coloneqq \left\langle \delta n\left(\vec{r},\Omega,t\right)\delta n\left(\overleftarrow{r}'\Omega'0\right)\right\rangle = \int d^3\vec{r}''d\Omega''$ $\chi\left(\vec{r},\vec{r}'',\Omega,\Omega'',t\right)\sigma\left(\vec{r}'',\vec{r}',\Omega'',\Omega'\right)$ whose dynamical evolution is attained from Eq. (4) after multiplying both sides by $\delta n\left(\vec{r},\Omega,t=0\right)$ and taking further an ensemble average. The resulting dynamical equation of the van Hove function has at t = 0 the initial condition $\int d^3\vec{r}''d\Omega''\sigma\left(\vec{r},\vec{r}'',\Omega,\Omega''\right)\chi\left(\vec{r}'',\vec{r}',\Omega'',\Omega',t=0\right) =$ $\sigma\left(\vec{r},\vec{r}',\Omega,\Omega'\right)$. The properties in Eq. (6) depend on the knowledge of the structure factor of the ferrofluid, which takes into account the micro-structural order of particles inside the ferrofluid as dictated by the underlying interaction potential. It is valid at high concentrations but ignores hydrodynamic interactions among particles. For monodisperse colloids, the tracer is equal to the other particles and the fluid is homogeneous. Thus, the distribution of particles is $n^{eq}(r,\Omega) =$ $\rho g\left(r=\left|\vec{r}\right|,\Omega,\Omega'(0,0)\right)$. Notice that the pair correlation function is defined between the tracer orientation $\Omega'(0,0)$, and another particle with $\Omega(\theta,\varphi)$, separated by the mean distance $r=\left|\vec{r}-\vec{r}'\right|$. Due to the spatial symmetry of the potential ψ, the pair correlation function has the rotationally invariant expansion $g(r,\Omega,\Omega') =$ $g(r)+h_\Delta(r)\Delta+h_D(r)D_1$, with $\Delta \coloneqq \hat{u}_1\cdot\hat{u}_2$, $D_1 \coloneqq \left[3\hat{\vec{r}}_{12}\cdot\hat{u}_1\hat{\vec{r}}_{12}\cdot\hat{u}_2-\hat{u}_2\cdot\hat{u}_1\right]$, where $\hat{\vec{r}} = \vec{r}/r$, $\hat{u}$ is the unitary dipole vector with orientation $\hat{u}=\hat{u}(\theta,\varphi)$. Using the Fick approximation for the Onsager coefficient, $L(r,r',\Omega,\Omega') = \rho\left[D^0\nabla^2+D_R^0\nabla_\Omega\right]$ $\delta(r-r')\delta(\Omega-\Omega')$, the unknown propagator in Eq. (4) $\chi = \exp\left(-tL\circ\sigma^{-1}\right)$, $\circ \coloneqq$ $\int d^3\,\vec{r}\,\,d\Omega$ can be fully determined. For a spherical particle, the free translational and rotational diffusion coefficients are $D^0=k_BT/\zeta^0$, $D_R^0=k_BT/\zeta_R^0$, with $\zeta^0=3\pi\eta_{sol}d$, $\zeta_R^0=\pi\eta_{sol}d^3$, and η_{sol} the solvent viscosity. Taking the Laplace transform $\Delta\zeta(\omega) =$ $\int_0^\infty dte^{i\omega t}\Delta\zeta(t)$ of the friction tensor in Eq. (6), it yields the real part of the translational and rotational diffusion coefficients of the tracer at the longtime overdamped regime $D=k_BT/\left[\zeta^0+\mathrm{Re}\Delta\zeta(\omega=0)\right]$, $D_R=k_BT/\left[\zeta_R^0+\mathrm{Re}\Delta\zeta_R(\omega=0)\right]$ [34], where

$$\mathrm{Re}\Delta\zeta = \frac{\zeta^0}{6\pi^2\rho^*}\int_0^\infty dx x^4\frac{\left(S_{,0}^{00}(x)-1\right)^2\tau_{s,iso}^*}{S_{,0}^{00}(x)} + \frac{128\pi\zeta^0\rho^*\mu^{*4}}{3}\int_0^\infty dx j_2(x)^2\left(6+x^2\right)\left[2\tau_{s,1}^{*2}+3\tau_{s,0}^{*2}\right], \tag{7}$$

$$\mathrm{Re}\Delta\zeta_R = \frac{128\pi\rho^*\mu^{*4}\zeta_R^0}{105}\int_0^\infty dx j_1(x)^2\left(6+x^2\right)\left[67\tau_{s,1}^{*2}+38\tau_{s,0}^{*2}\right],$$

j_l is the spherical Bessel function of order l, $\tau_{s,iso}^* = 1/\left[x^2\left(1+1/S_{,0}^{00}(x)\right)\right]$, $\tau_{s,\alpha}^* = S_{,\alpha}^{11}(x)/[8\pi(x^2+6)]$, $x \coloneqq kd$. The structure factor components of the dipolar liquid are

$$S_{,0}^{00}(x) = 1+\frac{\rho^*}{d^3}[g(x)-1],\ S_{,0}^{11}(x) = 1+\frac{\rho^*}{3d^3}[h_\Delta(x)+2h_D(x)],$$

$$S_{,1}^{11}(x) = 1+\frac{\rho^*}{3d^3}[h_\Delta(x)-h_D(x)]. \tag{8}$$

These correlation function components are obtained from the Fourier transform of their definitions

$$g(r) = \frac{\left\langle \sum_{i,\, j(i\neq j)} \delta\left(r - \left|\vec{r}_{ij}\right|\right)\right\rangle}{N 4\pi\rho^* r^2}, h_D(r) = \frac{3}{2}\frac{\left\langle \sum_{i,\, j(i\neq j)} \delta\left(r - \left|\vec{r}_{ij}\right|\right)\left[3\hat{\vec{r}}_{ij}\cdot\hat{u}_i\hat{\vec{r}}_{ij}\cdot\hat{u}_j - \hat{u}_i\cdot\hat{u}_j\right]\right\rangle}{N 4\pi\rho^* r^2},$$

$$h_\Delta(r) = 3\frac{\left\langle \sum_{i,\, j(i\neq j)} \delta\left(r - \left|\vec{r}_{ij}\right|\right)\hat{u}_i\cdot\hat{u}_j\right\rangle}{N 4\pi\rho^* r^2} \tag{9}$$

In **Figure 4,** Ref. [34] is provided a plot of the translational and rotational self-diffusion coefficients of such a theory. In this picture, we compare the diffusion coefficients with Langevin dynamics simulation results for the same diffusion coefficients by using typical parameters of $\mu^{*2} = \mu_0 m^2/\left(4\pi d^3 k_B T\right)$ for the real ferrofluid made of Fe_2O_3. μ_0 is the magnetic permeability of vacuum. The material data are: [40] $\varepsilon_0 = 5.45311 \times 10^{-23} J$, $d = 10^{-8} m$, particle mass and the viscosity are $m_0 = 2.70710 Kg$, $\eta_{sol} = 0.852 \times 10^{-3} Kg/ms$, respectively.

2.5 Diffusion microrheology of colloidal magnetic fluids under no external electric or magnetic fields

Ferrofluids are complex fluids whose viscoelastic response to weekly applied strain rates $\dot{\gamma}(t)$ is represented by a constitutive equation for the shear stress $\sigma(t) = \int_0^t dt' G(t-t')\dot{\gamma}(t)$ where the dot means time derivative and the shear modulus is $G(t)$. In the representation of frequency space ω, the shear is $\sigma(\omega) = G(\omega) i\omega\gamma(\omega)$. Mason and Weitz [49] assumed that the macroscopic temporal relaxation of $G(t)$ is the same time scale of the viscosity that affects a tracer particle that diffuses in the viscoelastic fluid. Because the shear stress divided by the strain rate has dimensions of viscosity, Mason et al. [49] defined the viscosity as $\eta(t) = \sigma(t)/\dot{\gamma}(t)$. Thus, they proposed that for spherical particles undergoing translational diffusion and in the frequency space, it is $G(\omega) = i\omega\eta(\omega) = i\omega\zeta(\omega)/3\pi d$ for a particle experiencing

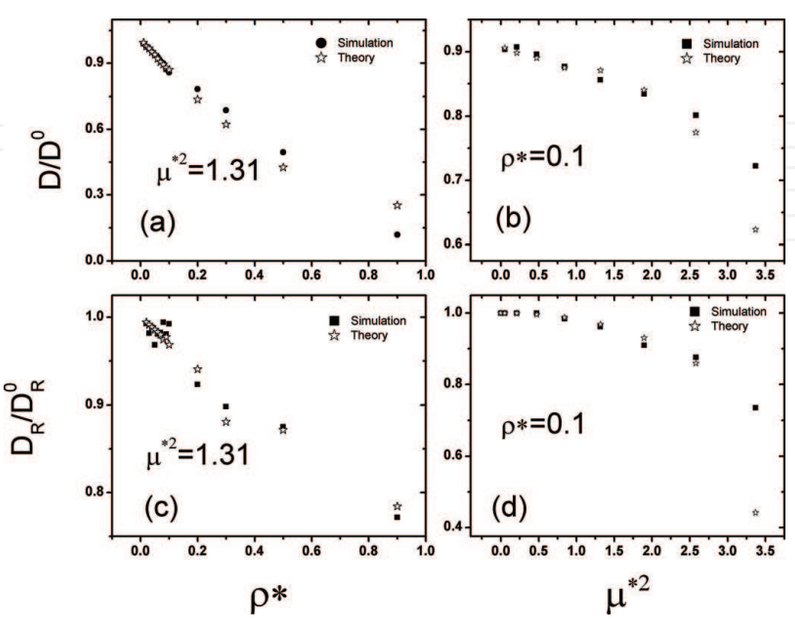

Figure 4.
Translational (rotational) self-diffusion coefficients D/D^0 $\left(D_R/D_R^0\right)$ versus density (a) ((c)), and dipole strength (b) ((d)). Simulation calculations are depicted with a black symbol and theory of Eq. (6) with ∘.

effective friction $\zeta(\omega)$. Here, we propose under the same conditions that the complex shear modulus of a ferrofluid is given by $G(\omega) = G' + iG'' = i\omega\left(\zeta^0 + \Delta\zeta(\omega)\right)/3\pi d = i\omega\eta(\omega)$. Since the complex viscosity of a viscoelastic media is defined by $\eta = \eta' - i\eta'$, we find for the elastic and dissipative moduli, respectively [34]

$$G'(w) = \omega\eta''(\omega) = \int_0^\infty dx \left[\frac{P_0^{00}(x)\left(\omega^*\tau^*_{s,iso}\right)^2}{1+\left(\omega^*\tau^*_{s,iso}\right)^2} + \frac{P_1^{11}(x)\left(\omega^*\tau^*_{s,1}\right)^2}{1+\left(\omega^*\tau^*_{s,1}\right)^2} + \frac{P_0^{11}(x)\left(\omega^*\tau^*_{s,0}\right)^2}{1+\left(\omega^*\tau^*_{s,0}\right)^2}\right],$$

$$G''(w) = \omega\eta'(\omega) = \frac{k_BT\omega^*}{3\pi d^3} + \int_0^\infty dx \left[\frac{P_0^{00}(x)\omega^*\tau^*_{s,iso}}{1+\left(\omega^*\tau^*_{s,iso}\right)^2} + \frac{P_1^{11}(x)\omega^*\tau^*_{s,1}}{1+\left(\omega^*\tau^*_{s,1}\right)^2} + \frac{P_0^{11}(x)\omega^*\tau^*_{s,0}}{1+\left(\omega^*\tau^*_{s,0}\right)^2}\right],$$

$$P_0^{00}(x) = \frac{k_BTx^4\left(S^{00}_{,0}(x)-1\right)^2}{18\pi^3d^3\rho^*S^{00}_{,0}(x)}, P_1^{11}(x) = -\frac{32k_BT\rho^*\mu^{*4}j_2(x)^2S^{11}_{,1}(x)}{9\pi d^3},$$

$$P_0^{11}(x) = \frac{48k_BT\rho^*\mu^{*4}j_2(x)^2S^{11}_{,0}(x)}{9\pi d^3}, \tag{10}$$

where $\omega^* = \omega t_B, t_B = d^2/D^0$. **Figure 5** provides a comparison of the viscoelastic moduli of Eq. (10) with Langevin dynamics simulations for the same parameter as those of **Figure 4**.

We notice that the effective viscosity at the overdamped regime $\omega = 0$, which results from Eq. (10), is $\eta_0 = t_BG_o$, where the storage modulus of the ferrofluid is $G_o = \left(k_BT/3\pi d^3\right)D^0/D$. At low volume fraction $\phi = \pi\rho^*/6$ of colloidal particles in the magnetic fluid, we found the following expression of the viscosity $\eta_0 \approx \eta_{sol}(1+5\phi/2)$, which is the known exact Einstein result for low volume fractions if we assume that the free parameter ζ^0 can be replaced by the approximated form proposed by Mazur and Geigenmüller $\zeta^0(1+1.5\phi)/(1-\phi)$ [50], which describes very well the free particle diffusion coefficient for all volume fractions.

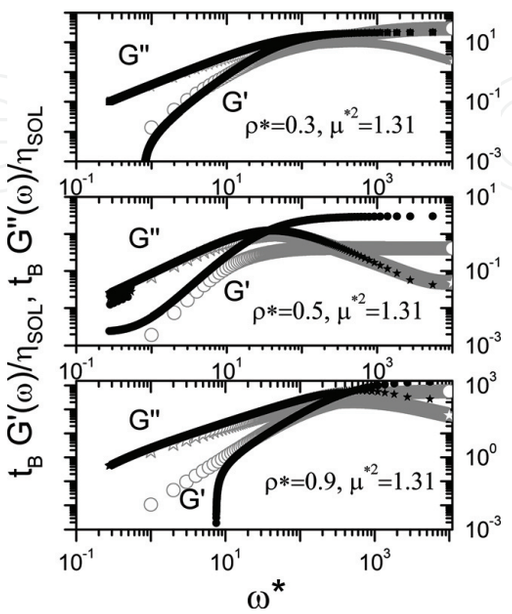

Figure 5.
Logarithmic plot of elastic G' and loss G'' moduli as a function of dimensionless frequency ω^* at three different concentrations and fixed dipole moment. Theory for $G'(G'')$ is denoted by $\circ(*)$ and that with simulation by $\bullet$, $*$.

2.6 Dynamic susceptibility response of a ferrofluid

The time-dependent magnetic susceptibility $\chi(t)$ of a ferrofluid can be measured either under a time-oscillating external magnetic field or in its absence with Altern Current dielectric spectroscopic techniques [51]. Our approach to calculating this property is based on the diffusion equation Eq. (4) that leads us to an expression for the collective dynamical property $\chi(t)$ regarding the friction Eq. (6). For this purpose, we multiplied Eq. (4) by $\delta n(t=0)\sum_{i,j}\hat{u}_i(t)\hat{u}_j(t)$, then we made a statistical average and Fourier transformed to write the dynamical equation of the collective magnetic tensor function

$$\langle M_k(t)M_{-k}(t=0)\rangle = -\left(m^2\mu_0 N/12\pi\right)C^{11}_{,1}(k,t),\ M_k(t) := \left(\mu\sqrt{\mu_0}/(4\pi)^{3/2}\right) \times \sum_{i=1}^{N}\int d^3\vec{r}\,e^{ik\cdot\vec{r}_i}(t)d\Omega\hat{u}_x(t)\delta n(r,\Omega,t), \tag{11}$$

where $C^{11}_{,1}$ is the transversal component of the van Hove function. We extended the hydrodynamic approach of Hess and Klein [52] to include rotational Brownian motion of the particles and derived the dynamical equation of the Van Hove function

$$\frac{\partial C(k,\Omega,t)}{\partial t} = \int_0^t dt' d\Omega' M(k,\Omega,\Omega',t-t')C(k,\Omega',t') \tag{12}$$

This equation is valid for colloidal suspensions of particles with axially symmetric potentials, where the memory function $M(k,\Omega,\Omega',t)$ is related to the friction Eq. (6), which does not require such an approximation on L [52]. The solution of this equation for the transversal component of the van Hove function $C(k,\Omega,t)$ leads to the complex susceptibility function in the frequency domain, and it is given by $\chi(k,\omega) = (4\pi\rho^*\mu^{*2}/3)\left[S^{11}_{,0}(x) - i\omega C^{11}_{,1}(x,\omega)\right] + 1$. This equation reproduces

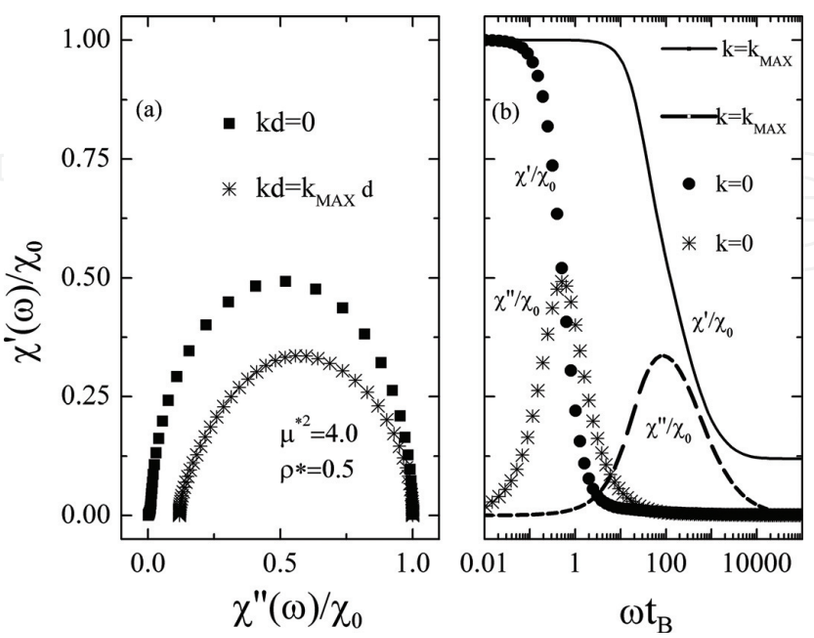

Figure 6.
Real χ' and imaginary χ'' magnetic susceptibilities of a ferrofluid normalized to the initial value of susceptibility χ_0. Picture (a) is a magnetic Cole-Cole plot and (b) depicts the susceptibility moduli versus frequency ω. The susceptibilities were evaluated at k_{max} the value of the wave number at the highest first peak of the structure factor, and $k = 0$.

similar results of a model molecular liquid of Wei and Patey [53] who, however, used a Kerr dynamical equation for C. Since $\chi = \chi' + i\chi''$ in **Figure 6**, we provide typical plots of the real and imaginary components of the magnetic susceptibility of the ferrofluid Fe_2O_3.

Alternative kinetics methods for low-density ferrofluids are given in [40].

3. Conclusion

This review highlights several active research lines on the structure and dynamics in ferrofluids. These investigations are motivated by many experimental observations that colloidal ferromagnetic particles both in bulk or in thin film aggregate, building several macroscopic structures of practical and scientific interest. As for all applications where colloidal materials are being processed, it is necessary to understand the interparticle interactions to have better control of the resulting structures and their properties. The interactions are known experimentally under specific conditions through the measured phase diagrams [11]; it has been found [29] that a useful potential that represents well the structure factor of ferrofluids is a Lennard-Jones plus dipolar interaction between pairs of particles. Therefore, our use of this potential in an evolutionary genetic algorithm leads to **Figure 1**, which shows transient metastable crystalline structures of a monodisperse ferrofluid at $T = 0K$. On the other hand, **Figure 2** shows the predicted structure factors using material parameters of typical Fe_2O_3 ferrofluid. There we observe that for low particle density and dipole moment, the particles are dispersed in the fluid, whereas for the highest dipole moment system, they form chains. As a consequence, there are noticeable effects on the collective diffusion coefficient as it is shown in **Figure 3,** where we notice that as the strength of the dipole moment is increased for low-density suspensions, this property drops because of particles' association in larger structures (chains). However, for higher-density suspensions, particles re-disperse again, therefore, increasing their collective diffusion. In Section 2.4, we presented the stochastic Langevin approach to describe the diffusion of a tracer particle in colloidal magnetic fluids. **Figure 4** provides theoretical predictions of this theory for the longtime translational and rotational self-diffusion coefficients Eq. (7) of a ferroparticle for the same material parameters of Fe_2O_3. We notice that the theory prediction has an agreement with Langevin dynamics simulations. In Section 2.5, we described our extension of a hydrodynamic theory of colloid dynamics [52] to include the rotational Brownian motions of ferrofluid's particles. As a result, we derived an equation of the complex susceptibility $\chi(k, w)$ that depends on the diffusion constants $D(\omega)$, $D_R(\omega)$ of a tracer particle in the colloid, which were given in Section 2.4. Thus, in **Figure 6,** we show the predicted magnetic Cole-Cole plot and real and imaginary components of the susceptibility moduli for Fe_2O_3 ferrofluid. There remain further studies to find the successful comparison of this method with well-characterized magnetic colloidal fluids and computer simulations in model ferrofluid systems.

Acknowledgements

The authors acknowledge the General Coordination of Information and Communications Technologies (CGSTIC) at CINVESTAV for providing HPC resources on the Hybrid Supercomputer "Xiuhcoatl" that has contributed to the research results reported within this chapter.

Conflict of interest

There are no conflicts to declare.

IntechOpen

Author details

Ricardo Peredo Ortíz[1], Martin Hernández Contreras[1*] and Raquel Hernández Gómez[2]

1 Physics Department, Center for Research and Advanced Studies of the National Polytechnic Institute, CD Mexico, Mexico

2 Computation Department, Center for Research and Advanced Studies of the National Polytechnic Institute, CD Mexico, Mexico

*Address all correspondence to: marther@fis.cinvestav.mx

IntechOpen

© 2018 The Author(s). Licensee IntechOpen. This chapter is distributed under the terms of the Creative Commons Attribution License (http://creativecommons.org/licenses/by/3.0), which permits unrestricted use, distribution, and reproduction in any medium, provided the original work is properly cited. CC BY

References

[1] Rosensweig RE. Ferrohydrodynamics. Cambridge: Cambridge University Press; 1985

[2] Jordan A, Scholz R, Maier-Hauff K, Johannsen M, Wust P, Nadobny J, et al. Presentation of a new magnetic field therapy system for the treatment of human solid tumors with magnetic fluid hyperthermia. Journal of Magnetism and Magnetic Materials. 2001;**225**:118-126

[3] Kim SH, Lee SY, Yang SM, Yi GR. Self-assembled colloidal structures for photonics. NPG Asia Materials. 2011;**3**: 25-33

[4] He L, Wang H, Ge J, Yin Y. Magnetic assembly route to colloidal responsive photonic nanostructures. Accounts of Chemical Research. 2012;**45**:1431-1440

[5] Andelman D, Rosensweig RE. Modulated Phases: Review and Recent Results. The Journal of Physical Chemistry. B. 2009;**113**:3785-3798

[6] Klapp SHL. Collective dynamics of dipolar and multipolar colloids: from passive to active systems. Current Opinion in Colloid & Interface Science. 2016;**21**:76-85

[7] Tierno P. Recent advances in anisotropic magnetic colloids: Realization, assembly and applications. Physical Chemistry Chemical Physics. 2014;**16**:23515-23528

[8] Schilling R, Scheidsteger T. Mode coupling approach to the ideal glass transition of molecular liquids: Linear molecules. Physical Review E. 1997;**56**: 2932-2949

[9] Snezhko A. Non-equilibrium magnetic colloidal dispersions at liquid–air interfaces: dynamic patterns, magnetic order and self-assembled swimmers. Journal of Physics: Condensed Matter. 2011;**15**:153101 (1-21)

[10] Ramírez-González PE, Medina Noyola M. Glass transition in soft-sphere dispersions. Journal of Physics: Condensed Matter. 2009;**21**:075101 (1-13)

[11] Yethiraj A, van Blaaderen A. A colloidal model system with an interaction tunable from hard sphere to soft and dipolar. Nature. 2003;**421**: 513-517

[12] Klokkenburg M, Erne BH, Meeldijk JD, Wiedenmann A, Pethukov AV, Dullens RPA, et al. In situ imaging of field-induced hexagonal columns in magnetite ferrofluids. Physical Review 36 Letters. 2006;**97**:185702 (1-4)

[13] Cousin F, Dubois E, Cabuil V. Tuning the interactions of a magnetic colloid suspension. Physical Review E. 2003;**68**:021405 (1-9)

[14] Pham AT, Zhuang Y, Detwiler P, Socolar JES, Charbonneau P, Yellen BB. Phase diagram and aggregation dynamics of a monolayer of paramagnetic colloids. Physical Review E. 2017;**95**:052607 (1-12)

[15] Hynninen AP, Dijkstra M. Phase Diagram of dipolar hard and soft spheres: Manipulation of colloidal crystal structures by an external field. Physical Review Letters. 2005;**94**: 138303 (1-4)

[16] Spiteri L, Messina R. Dipolar Crystals: The crucial role of the clinohexagonal prism phase. Physical Review Letters. 2017;**119**:155501 (1-4)

[17] Weis JJ, Levesque D. Advanced Computer Simulation Approaches for Soft Matter Sciences II. Berlin Heidelberg: Springer; 2005. pp. 163-225

[18] Wagner J, Fischer B, Autenrieth T. Field induced anisotropy of charged magnetic colloids: A rescaled mean spherical approximation study.

The Journal of Chemical Physics. 2006; **124**:114901 (1-10)

[19] Wagner J, Fischer B, Autenrieth T, Hempelmann R. Structure and dynamics of charged magnetic colloids. Journal of Physics: Condensed Matter. 2006;**18**:S2697-S2711

[20] Martin GAR, Bradbury A, Chantrell RW. A comparison between a three-dimensional Monte Carlo model and a hypernnetted chain approximation of a ferrofluid. Journal of Magnetism and Magnetic Materials. 1987;**65**:177-180

[21] Bradbury A, Martin GAR, Chantrell RW. Zero field particle correlations in a ferrofluid using Monte Carlo simulations and the hypernetted chain approximation. Journal of Magnetism and Magnetic Materials. 1987;**69**:5-11

[22] Hayter JB, Pynn R. Structure factor of a magnetically saturated ferrofluid. Physical Review Letters. 1982;**49**:1103-1106

[23] Pynn R, Hayter JB, Charles SW. Determination of ferrofluid structure by neutron polarization analysis. Physical Review Letters. 1983;**51**:710-713

[24] Bacri JC, Cebers A, Bourdon A, Demouchy G, Heegaard BM, Perzynski R. Forced rayleigh experiment in a magnetic fluid. Physical Review Letters. 1995;**74**:5032-5935

[25] Gazeau F, Dubois E, Bacri JC, Boue F, Cebers A, Perzynski R. Anisotropy of the structure factor of magnetic fluids under a field probed by small-angle neutron scattering. Physical Review E. 2002;**65**:031403 (1-15)

[26] Bacri JC, Cebers A, Bourdon A, Demouchy G, Heegaard BM, Kashevsky B, et al. Transient grating in a ferrofluid under magnetic field: Effect of magnetic interactions on the diffusion coefficient of translation. Physical Review E. 1995; **52**:3936-3942

[27] Meriguet G, Dubois E, Bourdon A, Demouchy G, Dupuis V, Perzynski R. Forced Rayleigh scattering experiments in concentrated magnetic fluids: effect of interparticle interactions on the diffusion coefficient. Journal of Magnetism and Magnetic Materials. 2005;**289**:39-42

[28] Lal J, Abernathy D, Auvray L, Diat O, Grubel G. Dynamics and correlations in magnetic colloidal systems studied by X-ray photon correlation spectroscopy. European Physical Journal E: Soft Matter and Biological. Physics. 2001;**4**: 263-271

[29] Meriguet G, Dubois E, Jardat M, Bourdon A, Demouchy G, Dupuis V, et al. Understanding the structure and the dynamics of magnetic fluids: coupling of experiment and simulation. Journal of Physics: Condensed Matter. 2006;**18**:S2685-S2696

[30] Meriguet G, Jardat M, Turq P. Structural properties of charge-stabilized ferrofluids under a magnetic field: A Brownian dynamics study. The Journal of Chemical Physics. 2004;**121**: 6078-6085

[31] Meriguet G, Jardat M, Turq P. Brownian dynamics investigation of magnetization and birefringence relaxations in ferrofluids. The Journal of Chemical Physics. 2005;**123**:144915 (1-8)

[32] Hernández-Contreras M, Ruíz Estrada H. Transport properties of ferrofluids. Physical Review E. 2003;**68**: 031202 (1-7)

[33] Peredo-Ortíz R, Hernández Contreras M, Hernández Gómez R. Diffusion in monodisperse ferrofluids. Journal of Physics: Conference Series. 2017;**792**:012099 (1-11)

[34] Peredo-Ortíz R, Hernández Contreras M. Diffusion microrheology of ferrofluids. Revista Mexicana de Fisica. 2018;**64**:82-93

[35] Mertelj A, Rešetič A, Gyergyek S, Markovec D, Čopič M. Anisotropic microrheological properties of chain-forming magnetic fluids. Soft Matter. 2011;**7**:125-131

[36] Yendeti B, Thirupathi G, Vudaygiri A, Singh R. Field-dependent anisotropic microrheological and microstructural properties of dilute ferrofluids. European Physical Journal E: Soft Matter and Biological Physics. 2014;**37**: 10 (1-8)

[37] Mazoyer S, Ebert F, Maret G, Keim P. Dynamics of particles and cages in an experimental 2D glass former. Europhysics Letters. 2009;**88**:66004 (1-6)

[38] Lacoste D, Lubensky TC. Phase transitions in a ferrofluid at magnetic-field-induced microphase separation. Physical Review E. 2001;**64**:041506 (1-8)

[39] de Gennes PG, Pincus PA. Pair correlations in a ferromagnetic colloid. Physics Kondens Matter. 1970;**11**:189-194

[40] Odenbach S. Colloidal Magnetic Fluids. 1st ed. Berlin: Springer; 2009

[41] Tlusty T, Safran SA. Defect-induced phase separation in dipolar fluids. Science. 2000;**290**:1328-1331

[42] Sreekumari A, Ilg P. Slow relaxation in structure-forming ferrofluids. Physical Review E. 2013;**88**:042315 (1-9)

[43] Russel WB, Saville DA, Showalter WR. Colloidal Dispersions. New York NY: Cambridge University Press; 1989

[44] Israelachvili JN. van der Waals dispersion force contribution to works of adhesion and contact angles on the basis of macroscopic theory. Journal of the Chemical Society, Faraday Transactions 2. 1973;**69**:1729-1738

[45] Fornleitner J, Loverso F, Kahl G, Likos CN. Genetic algorithms predict formation of exotic ordered configurations for two-component dipolar monolayers. Soft Matter. 2008; **4**:480-484

[46] Autenrieth T, Robert A, Wagner J, Grubel G. The dynamic behavior of magnetic colloids in suspension. Journal of Applied Crystallography. 2007;**40**: 5250-5253

[47] Pyanzina E, Kantorovich S, Cerda JJ, Ivanov A, Holm C. How to analyze the structure factor in ferrofluids with strong magnetic interactions: a combined analytic and simulation approach. Molecular Physics. 2009;**107**: 571-590

[48] Kirchoff T, Lowen H, Klein R. Dynamical correlations in suspensions of charged rodlike macromolecules. Physical Review E. 1996;**53**:5011-5022

[49] Mason TG, Weitz DA. Optical measurements of frequency-dependent viscoelastic moduli of complex fluids. Physical Review Letters. 1995;**74**:1250-1253

[50] Mazur P, Geigenmüller U. A simple formula for the short-time self-diffusion coefficient in concentrated suspensions. Physica A. 1987;**146**:657-661

[51] Roeben E, Roeder L, Teusch S, Effertz M, Deiters UK, Schmidt AM. Magnetic particle nanorheology. Colloid & Polymer Science. 2014;**292**:2013-2023

[52] Hess W, Klein R. Generalized hydrodynamics of systems of Brownian particles. Advances in Physics. 1983;**32**: 172-283

[53] Wei D, Patey GN. Rotational motion in molecular liquids. The Journal of Chemical Physics. 1989;**91**:7113-7129